

Cite this: *Sustainable Food Technol.*,  
2026, 4, 2076

# Development of multifunctional and sustainable starch/polyvinyl alcohol–polyethylene glycol copolymer films reinforced with green tea extract for food packaging

Neha Rana,<sup>ab</sup> Ruchika<sup>ab</sup> and Ankit Saneja <sup>\*ab</sup>

This study explores a sustainable alternative to conventional plastic packaging by developing biodegradable films from starch (ST), a polyvinyl alcohol–polyethylene glycol (PVA–PEG) copolymer and green tea extract (TE) as a functional additive. The incorporation of TE at 0.5% w/v was demonstrated to significantly enhance the tensile strength ( $4.7 \pm 0.3$  MPa) and water contact angle ( $70.7 \pm 0.3^\circ$ ) of STKTE 0.5% film in comparison to a blank STKB film. The developed films also demonstrated significant improvement in barrier attributes, including UV-shielding (100%), water vapour and oxygen transmission. Further, the films were analysed using several techniques, including scanning electron microscopy (SEM), 3D optical profilometry, Fourier transform infrared spectroscopy (FTIR), X-ray diffraction (XRD) and thermogravimetric analysis (TGA). The results demonstrated that incorporating TE improved the structure, intermolecular interactions and thermal stability of the film. DPPH assay and cytocompatibility (95%) with L929 fibroblast cells confirmed the strong antioxidant properties and biocompatibility of the developed film, respectively. The incorporation of TE enhanced the antibacterial potential of the films, with significant inhibition of *Escherichia coli* and *Staphylococcus aureus*. The application of the developed films in the preservation of fresh cut apple cubes demonstrated reduced browning index, weight loss and pH, indicating better preservation compared to the blank film. Finally, the biodegradability of the film was assessed using soil burial tests, demonstrating a residual area of  $0.6 \pm 0.6\%$  within 10 days. These results highlight the potential of ST/PVA-PEG/TE films as eco-friendly, functional packaging materials to improve food shelf life while ensuring safety and sustainability.

Received 31st October 2025  
Accepted 8th January 2026

DOI: 10.1039/d5fb00838g

rsc.li/susfoodtech

## Sustainability spotlight

This study advances sustainable packaging by creating biodegradable starch/PVA–PEG copolymer films infused with green tea extract (TE). By replacing petroleum-based plastics with renewable, compostable materials, the films may reduce plastic pollution and dependence on fossil resources. Their natural antioxidant and antibacterial properties extend food shelf life, decreasing food waste. This innovation directly supports UN Sustainable Development Goals 12 (Responsible Consumption and Production), 13 (Climate Action), and 14 (Life Below Water) by promoting circular material use, mitigating environmental impact, and protecting ecosystems from plastic contamination. Overall, the work exemplifies a holistic approach to developing eco-friendly packaging solutions for a more sustainable future.

## 1. Introduction

Increasing concerns about plastic pollution have intensified the quest for sustainable packaging solutions for food preservation which are environment friendly.<sup>1,2</sup> Traditional petroleum-based plastics remain in the environment for decades, collecting in landfills and waterways, which has stimulated interest in renewable and biodegradable options that align with circular-economy

principles. Biopolymer films are particularly notable as they can provide food protection while minimizing long-term environmental impact when properly disposed of.<sup>3,4</sup> Starch (ST), an abundant and cost-effective polysaccharide, is a primary focus for biodegradable food packaging due to its effective film-forming capacity and natural compostability. ST-based films are widely used in different food applications due to their desirable features, such as high transparency, good sensory qualities, and excellent gas barrier properties.<sup>5,6</sup> However, their broader application in food packaging is hindered by drawbacks like low water resistance and weak mechanical strength. A promising approach to enhance their performance is to develop blend films by incorporating starch polymers with other compatible polymers.<sup>7–9</sup>

<sup>a</sup>Formulation Laboratory, Dietetics and Nutrition Technology Division, CSIR-Institute of Himalayan Bioresource Technology, Palampur 176061, Himachal Pradesh, India. E-mail: ankit.saneja@csir.res.in; ankitsaneja.ihbt@gmail.com; Tel: +91-1894-233339

<sup>b</sup>Academy of Scientific and Innovative Research (AcSIR), Ghaziabad 201002, India



By blending starch with other polymers, the films may gain enhanced strength and integrity, while polyethylene glycol (PEG) serves as a plasticizer for improving flexibility.<sup>7,10,11</sup> To further enhance functionality beyond simple physical protection, researchers are increasingly integrating natural bioactive materials into biopolymer matrices. Green tea extract (TE), rich in catechin polyphenols, is recognized for its antioxidant and antimicrobial properties, making it effective in combating oxidation and inhibiting foodborne pathogens.<sup>12,13</sup> The incorporation of TE into biodegradable films has been shown to improve their radical-scavenging activity and provide antibacterial benefits essential for extending shelf life and ensuring food safety.<sup>13–16</sup>

Therefore, this study focuses on developing a ST/PVA–PEG copolymer film that incorporates TE, aiming to combine biodegradability with inherent antioxidant and antibacterial functions (Fig. 1). The main objective was to present a sustainable alternative to conventional plastics that also actively contributes to maintaining food quality. Furthermore, instead of utilizing an external plasticizer, the PVA–PEG copolymer was utilized, which has intrinsic plasticizing properties. This approach provides the advantage of eliminating the extra optimization step needed for an external plasticizer to avoid the leaching phenomenon in the films. Furthermore, the PVA–PEG copolymer is well known for its excellent film forming ability and commonly utilized in the pharmaceutical industry.<sup>17</sup> Beyond functional improvements, the selection of bioactive ingredients and polymer blends involved the consideration of biocompatibility and safety for food contact, which is crucial for packaging. A thorough characterization investigation based on mechanical and surface properties was carried out to analyse the influence of TE on the structure and properties of the films. The morphology and surface topography were analysed using scanning electron microscopy (SEM) and 3D optical profilometry, respectively. The chemical interactions and molecular ordering were studied through Fourier-transform infrared spectroscopy (FTIR) and X-ray diffraction (XRD) to understand hydrogen bonding and crystallinity modifications within the ST/PVA–PEG/TE matrix. Additionally, thermogravimetric analysis (TGA) was utilized to determine thermal stability and degradation behaviour under heat, key attributes concerning processing and usability. The functional performance was evaluated through DPPH radical scavenging, to measure oxidative protection capabilities along with migration studies. The cytocompatibility of the developed films was assessed through fibroblast (L929) cell viability tests to confirm the safety. Further, the antibacterial activity was also analysed against common foodborne pathogens, including *Escherichia coli* and *Staphylococcus aureus*, using the colony forming unit methodology. To demonstrate practical applicability, the films were utilized for the packaging of fresh-cut apples, which are susceptible to enzymatic browning, moisture loss, weight loss, and pH change of the fruit.

## 2. Experimental

### 2.1. Materials

Potato starch (ST) was purchased from Central Drug House Limited (India). Kollicoat® IR (PVA–PEG copolymer) and DPPH were obtained from Sigma-Aldrich. All other reagents used were

of analytical grade. L929 fibroblast cells were obtained from NCCS, Pune, India. The two bacterial strains [*Escherichia coli* (MTCC 43) and *Staphylococcus aureus* (MTCC 96)] were procured from MTCC, India.

### 2.2. Preparation of green tea extract

The green tea was collected from the institutional tea processing facility. The green tea extract (TE) was prepared by adding 5 g of green tea to 500 mL of distilled water and heating at 80 °C for 20 min with continuous stirring. The obtained solution was then filtered to remove any residues. The filtrate was condensed using a rotatory evaporator (RV10, IKA, Germany) at 40 °C followed by freeze-drying.<sup>13,18</sup> The extract was removed with help of a spatula and ground to obtain the green tea extract powder. The total phenolic content (TPC) of the TE was estimated *via* the Folin–Ciocalteu method and expressed as gallic acid equivalents in mg g<sup>-1</sup> of dry weight of the TE.<sup>19</sup> The TPC of all the samples was assessed in three replicates, and the average value was reported.

### 2.3. Preparation of starch/PVA–PEG/green tea extract films (STKTE films)

The different film forming solutions were prepared by blending ST and the PVA–PEG co-polymer (KIR) as the primary film base using the solvent casting method.<sup>18</sup> Briefly, starch (6% w/v) and PVA–PEG co-polymer (11% w/v) were dissolved in distilled water with continuous stirring at 60 °C, in two separate beakers. Once completely dissolved, the solutions were combined in a 1:1 ratio (v/v) and stirred for another 30 min. The tea extract (TE) at different concentrations (0.25, 0.5 and 1% w/v) was added to the primary film base to obtain three different films: (i) ST/KIR/TE (0.25% w/v) film (STKTE 0.25%); (ii) ST/KIR/TE (0.5% w/v) film (STKTE 0.5%); and (iii) ST/KIR/TE (1% w/v) films (STKTE 1%). The obtained homogeneous solutions were cast on a flat surface with a digital adjustable applicator (VJ Instruments, India) to obtain films of uniform thickness. The films were dried at room temperature and stored till further use. A blank film (STKB) was also prepared, consisting of starch and the PVA–PEG copolymer only. The thickness of the films were determined using a digital micrometer and expressed in mm (millimetres).

### 2.4. Optimization of the STKTE films

**2.4.1. Film mechanical attributes.** The tensile strength (TS) and elongation at break (EAB) of the developed film samples were measured using a tensile tester (SSIC-TTM-50 kgf-SC, SISCO, India). Prior to testing, the film samples were cut into 100 mm × 20 mm strips and tested at a specific force rate.

**2.4.2. Water contact angle (WCA).** The WCA was measured using a DMe-211 Plus contact angle meter (Kyowa, Japan) following the sessile drop method.<sup>20</sup> Before the experiment, the film samples (20 × 20 mm) were placed flat on the sample stage, and a droplet (2 ± 0.1 μL) of distilled water was deposited carefully on the film sample. The contact angle was recorded immediately after deposition followed by capturing of images and analyzed using FAMAS software.



## 2.5. Solid state characterization and barrier property analysis of STKB and STKTE 0.5% films

**2.5.1. Scanning electron microscopy (SEM).** The surface morphologies of the STKB and STKTE 0.5% films were examined using a scanning electron microscope (SEM, Hitachi S-3400 N, 15 kV). The film samples (10 × 10 mm) were fixed on metal stubs with the help of adhesive carbon tape and sprayed with gold to ensure conductivity and clear imaging.<sup>20,21</sup>

**2.5.2. 3D optical profilometry.** The topology and roughness of the STKB and STKTE 0.5% film samples were examined using an optical profilometer (Contour GT-K, Bruker AXS, USA) operated in confocal mode.<sup>22</sup>

**2.5.3. Colour and UV-shielding analysis.** A UV-visible spectrophotometer (GENESYS™ 180, Thermo Scientific, USA), was used to determine the transmittance of the STKB and STKTE 0.5% film samples. The transmission spectrum was recorded in the range of 200–800 nm.<sup>23</sup> The color parameters  $L^*$  (lightness),  $a^*$  (red/green),  $b^*$  (yellow/blue) and  $\Delta E$  (total color difference) of the films were evaluated using a color reader (CR6, China).

**2.5.4. Fourier transform infrared spectroscopy (ATR-FTIR).** The possible molecular interaction between ST, PVA-PEG (KIR), TE, STKB and STKTE 0.5% films was studied by using an infrared spectrophotometer (Agilent Technologies, USA). The spectra were recorded at wavenumbers ranging from 500 to 4000  $\text{cm}^{-1}$ .<sup>24</sup>

**2.5.5. X-ray diffraction (XRD).** The crystallinity of ST, PVA-PEG (KIR), TE, STKB and STKTE 0.5% films was examined with an X-ray diffractometer (Malvern Panalytical diffractometer, UK). The diffraction patterns were recorded over a  $2\theta$  range of  $5^\circ$  to  $40^\circ$ .<sup>5</sup>

**2.5.6. Thermogravimetric analysis (TGA).** The thermal properties of ST, PVA-PEG, TE, and STKB STKTE 0.5% films were analyzed with a thermogravimetric analyzer (TA Instruments Discovery Series TGA5500 (Waters, USA)). In brief, a small amount of the sample was placed into a pan and heated from  $25^\circ\text{C}$  to  $550^\circ\text{C}$  at a rate of  $20^\circ\text{C min}^{-1}$  under a nitrogen flow and the % weight was recorded.<sup>25</sup>

**2.5.7. Opacity, moisture content, and barrier properties of STKB and STKTE 0.5% films.** The opacity of the STKB and STKTE 0.5% film samples was analysed by recording the absorbance using a UV-visible spectrophotometer (GENESYS™ 180 UV-spectrophotometer, Thermo Scientific, USA) at a specific wavelength of 500 nm.<sup>26</sup> The opacity was deduced using the following equation:

$$\text{Opacity of films} = A_{500} \times t \quad (1)$$

where  $A_{500}$  is the absorbance of the film samples and  $t$  is the thickness of the film (mm).

The % moisture content of the STKB and STKTE 0.5% films was evaluated using a UniBloc moisture analyzer (MOC 63u, Shimadzu, Japan). The water vapour permeability (WVP) of the film samples was tested by following the ASTM E96 standard method using Payne permeability cups (Raj Make, India).<sup>27</sup> Initially, the test cups were filled with 3 mL of distilled water,

sealed with films and placed in a vacuum desiccator for 24 h. The change in weight (g) of the test cups was recorded and the WVP was calculated.

$$\text{Water vapor permeability of films} = \frac{\Delta W \times X}{A \times t \times \Delta P} \quad (2)$$

where  $\Delta W$  represents the test cup weight change (g),  $X$  is the film thickness (mm),  $A$  corresponds to the film area ( $\text{m}^2$ ),  $t$  is the time period (s), and  $\Delta P$  is the water vapor pressure difference (Pa).

An indirect method was used to analyse the oxygen transmission across the film.<sup>28</sup> Briefly, centrifuge tubes containing 3 g of deoxidizer (iron powder) were sealed with films and placed at  $25^\circ\text{C}$ , and weighed after 48 h. The oxygen permeability (OP) of the films was determined using the following equation:

$$\text{Oxygen permeability} (10^{-6} \text{ g mm m}^{-2} \text{ s}^{-1}) = (\Delta m \times d)/(A \times t)(3)$$

where  $\Delta m$  is the mass change (g) of the tube,  $d$  is the film thickness (mm),  $t$  is the time (s) and  $A$  denotes the permeation area ( $\text{m}^2$ ).

## 2.6. Determination of the antioxidant activity of STKB and STKTE 0.5% films

The antioxidant activity of the STKB and STKTE 0.5% films was estimated using 2,2-diphenyl-1-picrylhydrazyl (DPPH) assay.<sup>13,21</sup> Briefly, 1 mL of film concentrations (125, 250, 500, 750, and 1000  $\mu\text{g mL}^{-1}$ ) was added to 2 mL of DPPH solution, vortexed, and incubated in the dark for 30 min. The absorbance at 517 nm was determined using a UV-spectrophotometer (GENESYS™ 180, Thermo Scientific, USA) and the % radical scavenging activity of the films was deduced using the equation:

$$\% \text{ scavenging activity of films} = \left( \frac{A_0 - A_1}{A_0} \right) \times 100\% \quad (4)$$

where  $A_0$  and  $A_1$  denote the absorbance of the blank DPPH solution and absorbance of the solution with the film sample, respectively.

## 2.7. Migration study of tea extract in STKTE 0.5% films

The migration behaviour of the TE incorporated in the STKTE 0.5% film was estimated using the total immersion method with three different simulants (water, 3% acetic acid and 95% ethanol)<sup>29</sup>. In short, film samples (1 × 3 cm) were immersed in 5 mL of simulant and incubated in the dark at  $40^\circ\text{C}$  for a period of 10 days. After incubation, the absorbance of the samples at 268 nm was recorded and the migrated TE content was deduced using a calibration curve of TE. Moreover, the antioxidant activity of the solution obtained after the migration test was also estimated using DPPH assay.

## 2.8. Biocompatibility of STKB and STKTE 0.5% films

Murine fibroblast cells (L929 cells) were utilized to assess the biocompatibility of STKB and STKTE 0.5% films.<sup>24,30</sup> Briefly, the L929 cells were seeded and treated with different film



concentrations (5, 25, 50, 75 and 100  $\mu\text{g mL}^{-1}$ ) for 24 h at 37 °C. The MTT assay was used to assess the effect of the films on the L929 cells and the % cell viability was calculated using the following equation:

$$\begin{aligned} & \% \text{ cell viability of fibroblast cells} \\ & = \left( \frac{\text{absorbance of sample}}{\text{absorbance of control}} \right) \times 100 \end{aligned} \quad (5)$$

In addition, the cells were subjected to staining using a Live/Dead™ Cell Imaging Kit (Invitrogen, Thermo Fisher Scientific) after treatment with the films (100  $\mu\text{g mL}^{-1}$  concentration). Images of fibroblast cells were captured using the ZOE™ Fluorescent Cell Imager (Bio-Rad) to determine live and dead cells.<sup>31</sup>

### 2.9. Antibacterial assessment of STKB and STKTE 0.5% films

The antibacterial efficacy of STKB and STKTE 0.5% films was assessed against two bacterial strains, *viz.* *E. coli* (Gram-negative) and *S. aureus* (Gram-positive).<sup>28</sup> Prior to the experiment, the film samples were sterilized *via* UV light treatment for 30 min. Further, sterilized film samples (20 mg  $\text{mL}^{-1}$ ) were dissolved in 25 mL of liquid medium inoculated with either *E. coli* (Luria broth) or *S. aureus* (nutrient broth) and incubated for 12 h (at 37 °C) with continuous agitation. The OD values of the samples were observed at specific intervals (1, 2, 4, 6, 8, 10 and 12 h) and after incubation the diluted (6-fold) bacterial suspension (100  $\mu\text{L}$ ) was uniformly spread over the sterile agar plates. The colonies were counted with the help of a Handheld Digital Colony Counter (HIMEDIA). The bacterial suspension without the film sample was considered as a control. The number of colonies counted was expressed in CFU per mL using the following equation:

$$\begin{aligned} & \text{Colony forming units per mL of film samples} \\ & = \frac{(\text{no. of colonies} \times \text{dilution factor})}{\text{volume of culture plated}} \end{aligned} \quad (6)$$

### 2.10. Application in fresh cut apple preservation

Apple preservation was assessed using STKB and STKTE 0.5% films to estimate their potential in maintaining the shelf life and quality of apples during storage. Fresh apples were procured from the local market at Palampur (HP), washed thoroughly and cut into cube shaped pieces (2 × 2 cm). The apple cubes were divided into four groups (in triplicate with 3 apple cubes in each replicate), *viz.* Group 1: uncovered (control); group 2: covered with conventional polyethylene packaging (PE); group 3: covered with STKB film; and group 4: covered with STKTE 0.5% film. The fresh cut apples were stored at room temperature for a period of 5 days. All groups were analysed during the storage period for weight loss (%), pH, and visual appearance.<sup>32</sup> For visual appearance, images were captured at regular time intervals. The % weight loss was calculated using the equation:

$$\text{Weight loss (\%)} \text{ of apple cubes} = \left( \frac{W_i - W_d}{W_i} \right) \times 100 \quad (7)$$

where  $W_i$  and  $W_d$  are the initial weight and weight on a specific day of the apple cubes, respectively.

The color parameters ( $L^*$ ,  $a^*$  and  $b^*$  values) of the apple cubes were measured using a colorimeter (CR-6, 3nh Technology, China) at different time points during storage. The browning index (BI) was evaluated to determine the browning degree of the apple cubes during the preservation period.<sup>33</sup> The BI of the apple cubes was calculated according to the following equation:

$$\text{BI of fresh cut apple} = \frac{y - 0.31}{0.172} \times 100 \quad (8)$$

$$\text{where } y = \frac{a + 1.75L}{5.645L + a - 3.02b} \quad (9)$$

### 2.11. Soil burial test assessment of STKB and STKTE 0.5% films

The STKB and STKTE 0.5% films' physical disintegration was estimated by soil burial testing.<sup>34</sup> Briefly, the film samples STKB and STKTE 0.5% (2 × 2 cm) were placed between mesh layers and buried at a depth of 10 cm in the soil. The films were regularly monitored and photographed at specific time intervals for a period of 10 days. The residual area of the film samples was measured using ImageJ software and calculated using the following equation:

$$\% \text{ residual film area} = \left( \frac{\text{residual area of the film}}{\text{initial area of the film}} \right) \times 100 \quad (10)$$

### 2.12. Statistical analysis

The statistical analysis of the obtained results was performed using GraphPad Prism 10 (GraphPad Software Inc., CA, USA). The *t*-test and one-way or two-way analysis of variance (ANOVA), followed by Tukey's post-hoc test were employed to compare differences between the groups with statistical significance considered at  $p < 0.05$ . All results were expressed as mean ± standard deviation (SD).

## 3. Results and discussion

### 3.1. Optimization and selection of tea extract incorporated ST/PVA-PEG copolymer/TE (STKTE) film

Starch-based packaging films have attracted considerable interest as eco-friendly alternatives to petroleum-based plastics due to their biodegradability, renewability, and cost-effectiveness. However, films composed solely of starch often face several limitations, such as high brittleness, inadequate mechanical strength, and significant hydrophilic tendencies, which lead to increased moisture sensitivity and reduced water resistance.<sup>6,22,35–38</sup> These challenges limit their direct application in food packaging and other uses that require flexibility, durability, and moisture stability. To overcome these issues, a PVA-PEG copolymer was integrated into a starch matrix. This copolymer has inherent plasticizing properties because of its flexible ether linkages and hydroxyl groups, which may enhance intermolecular hydrogen bonding and facilitate chain mobility.<sup>22,39</sup>



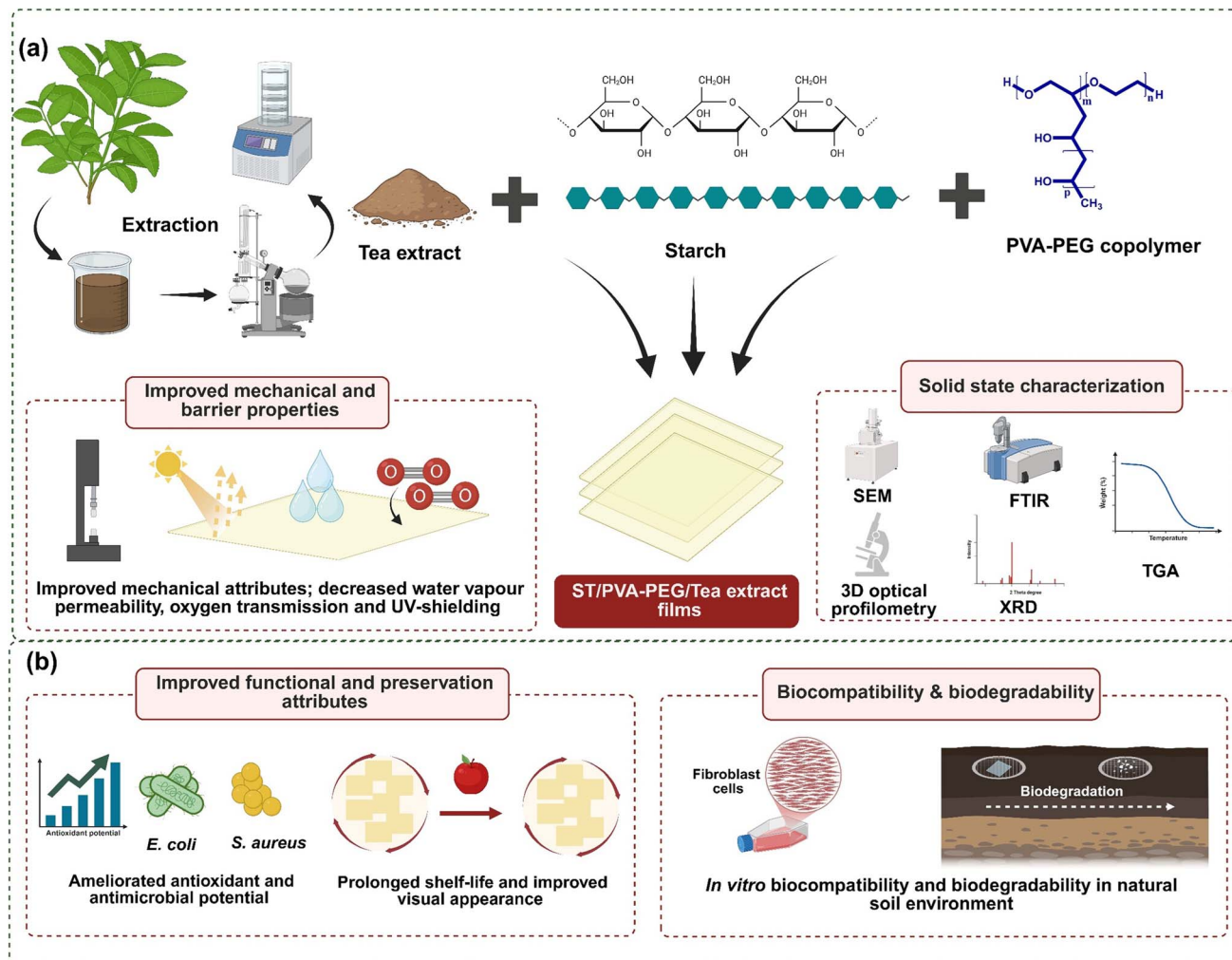


Fig. 1 (a) Schematic illustration of the development of a starch/PVA-PEG copolymer packaging film reinforced with green tea extract and its mechanical, barrier and solid-state characterization. (b) The developed film was further analysed in terms of its functional properties including antioxidant and antimicrobial properties, postharvest apple preservation, biocompatibility and biodegradability.

Further, TE was incorporated as a functional additive to impart additional active properties and reinforce the film structure. The TE, rich in polyphenolic content ( $458.9 \pm 0.5$  mg GAE per g), can form strong interactions with polymeric chains through hydrogen bonding and hydrophobic interactions.<sup>19,40–43</sup> The addition of such extracts impacts the film's mechanical and barrier properties in a multifaceted manner. Therefore, the ST/PVA-PEG/TE films were optimized based on tensile strength, elongation at break and water contact angle with varying concentrations of TE. The TE was incorporated in three different concentrations (w/v) into the polymeric solution, which resulted in the formation of three different types of films, viz. STKTE 0.25%, STKTE 0.5%, and STKTE 1% (Fig. 2).

The blank film composed of only ST and the PVA-PEG copolymer demonstrated a TS of  $2.2 \pm 0.9$  MPa, EAB of  $1.7 \pm 0.5\%$ , and WCA of  $58.6 \pm 0.6^\circ$ . The addition of TE in the polymeric matrix impacts the mechanical and WCA in a bell-shaped manner.<sup>22,24,42</sup> Specifically, the film with the lowest concentration of TE (STKTE 0.25%) exhibited the lowest TS ( $1.03 \pm 0.4$  MPa), EAB ( $2.2 \pm 0.5\%$ ), and WCA ( $60.9 \pm 5.4^\circ$ ). Furthermore,

significant enhancements in the mechanical properties as well as WCA of the film were observed in the film with 0.5% TE (STKTE 0.5%), which showed a TS of  $4.7 \pm 0.3$  MPa, EAB of  $3.8 \pm 1.2\%$ , and WCA of  $70.7 \pm 0.3^\circ$ , indicating enhanced intermolecular interaction between the TE and film components.<sup>22</sup> However, with a further increase in the TE amount (STKTE 1%), the mechanical performance and WCA decreased, which might be due to saturation and agglomeration. Conclusively, the STKTE 0.5% film demonstrated enhanced mechanical and WCA parameters, and was therefore selected for further experiments.

### 3.2. Characterization of the developed ST/PVA-PEG copolymer/TE (STKTE) film

**3.2.1. Surface and morphological analysis of the STKB and STKTE 0.5% film.** SEM and 3D profilometry analysis was conducted to observe the surface morphology and microstructural variations before and after incorporation of TE in the film (Fig. 3). The SEM analysis reveals that the morphology shifts from larger, irregular domains in the pure STKB film to smaller, more



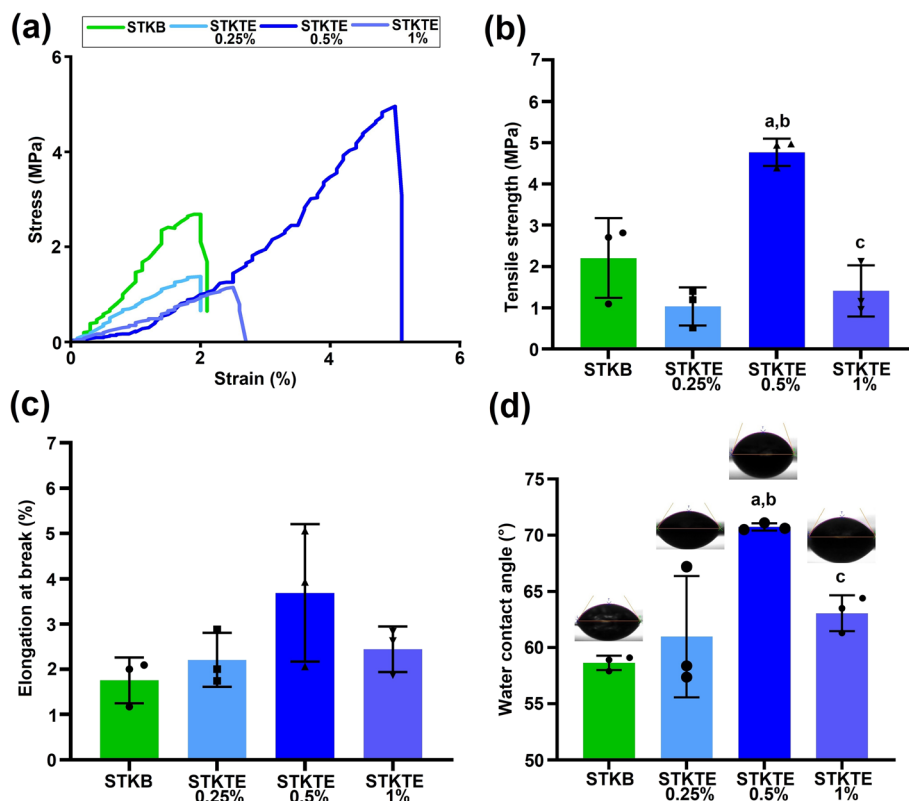


Fig. 2 The mechanical and surface properties of STKB and STKTE films with varying concentrations of green tea extract (TE). (a) Representative stress–strain curves demonstrate the mechanical behavior of the film samples. (b) Tensile strength, (c) elongation at break, and (d) water contact angle were measured for STKB and STKTE films containing 0.25%, 0.5%, and 1% w/v of TE. Data are presented as mean  $\pm$  standard deviation ( $n = 3$ ). Statistically significant differences are indicated by different letters above the bars: "a" denotes a significant difference from STKB, "b" from STKTE 0.25%, and "c" from STKTE 0.5%. In the graph d), representative images of water droplets showing WCA of film samples above the corresponding bar.

uniformly distributed domains in the STKTE 0.5% film, suggesting improved dispersion or interaction at the microscopic level. Further, the optical profilometry data demonstrated a slight increase in the average peak height ( $R_{pm}$ :  $6.5 \pm 2.4 \mu\text{m}$ ) and  $R_z$  (roughness of film) value ( $37.9 \pm 5.4 \mu\text{m}$ ) in the STKTE 0.5% film in comparison to the STKB film ( $R_{pm}$ :  $3.9 \pm 1.1 \mu\text{m}$  and  $R_z$ :  $33.2 \pm 6.3 \mu\text{m}$ ). The  $R_{pm}$  and  $R_z$  values provide essential information on surface roughness, which directly influences the mechanical integrity, wettability, and overall uniformity of food packaging films. Lower values of  $R_z$  indicate a smooth and uniform film surface, which is generally important for ideal packaging film.<sup>44</sup> These combined changes in the SEM and optical profilometry suggest that TE modifies the microstructure of the film, leading to enhanced surface texture and altered optical properties.<sup>6,45</sup>

**3.2.2. Optical and barrier attribute analysis of the STKB and STKTE 0.5% film.** Colour, opacity and light transmittance are crucial parameters for packaging film applications, as these impact on the product freshness and consumer perception. A higher opacity value indicates greater absorption of visible light by the film at a specific thickness, thereby reducing light transmission through the film. The addition of TE changes the color of the film and also impacts the % transmittance and opacity of the film (Fig. 4). The colorimetric analysis revealed that the STKTE 0.5% sample exhibits a noticeable yellow

coloration, with high  $b^*$  value (42.90) and positive  $a^*$  value (17.24), along with a lower lightness value ( $L^* = 51.92$ ) compared to the almost colorless STKB sample ( $L^* = 87.89$ ). The large color difference ( $\Delta E = 51.16$ ) between the two samples confirms the visible color change upon TE addition.<sup>6</sup>

Ultraviolet (UV) radiation significantly contributes to the deterioration of food quality; hence, packaging films should offer sufficient transparency while effectively blocking UV light to ensure product preservation. The UV-blocking capability of the films was assessed using a UV spectrophotometer.<sup>13</sup> The results revealed that the STKTE 0.5% film completely absorbed light in the UV region (UVA, UVB and UVC light) and demonstrated negligible transmittance across the film. This remarkable UV blocking ability of the STKTE 0.5% film was due to the polyphenolic constituents present in the TE which effectively absorb ultraviolet radiation.<sup>40,46</sup> The incorporation of 0.5% TE into STKB not only improves UV protection but also imparts a distinct yellow tint and reduces the lightness of the film. Similarly, the STKTE 0.5% film showed a high opacity value of  $0.039 \pm 0.00007$  compared to the STKB film ( $0.028 \pm 0.0002$ ) (Fig. 5a). This confirms that in the STKTE 0.5% film, the addition of the TE improved the light absorbing properties.

Further, the ability of packaging films to restrict the transmission of water and gases is a critical determinant of their



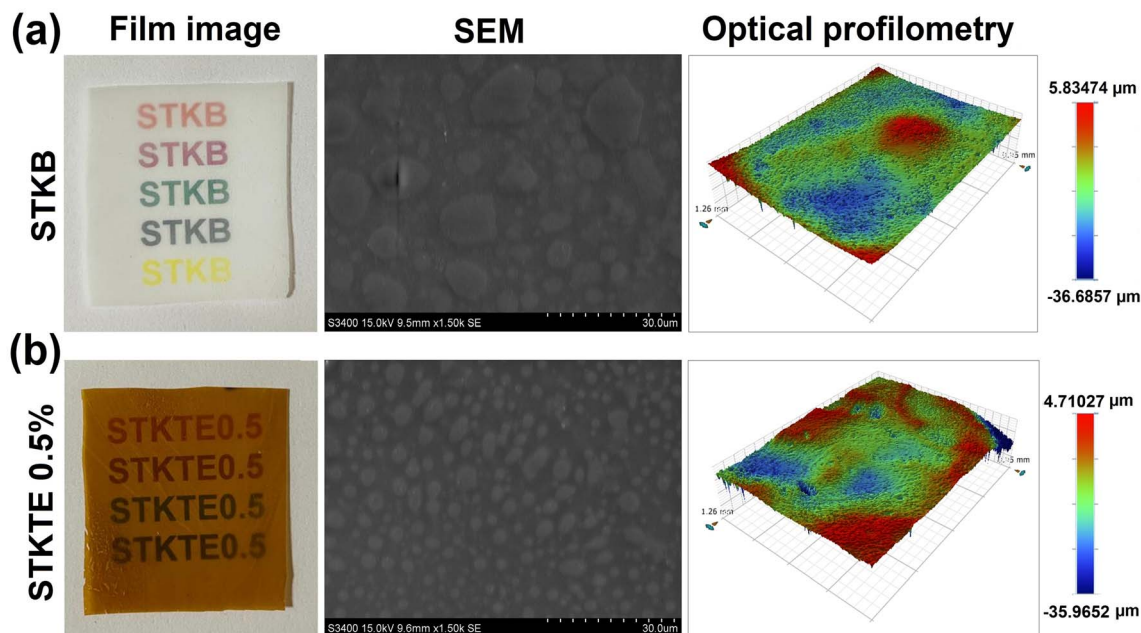


**Fig. 3** The film images, surface morphology, and topography of STKB and STKTE 0.5% films. The STKB film (a) appears highly transparent in the photographic image, allowing clear visibility of printed text under it. The corresponding SEM image reveals a relatively smooth surface with some dispersed features. Optical profilometry of the STKB film shows a moderately uniform surface with height variations ranging from  $-36.6857 \mu\text{m}$  to  $5.83474 \mu\text{m}$ . In contrast, the STKTE 0.5% film (b) shows a distinct yellowish tint in the photographic image and reduced transparency. The SEM image at the same magnification indicates a more heterogeneous surface with more irregular features, suggesting increased surface roughness. This is further confirmed by the optical profilometry data, which reveals a less uniform surface topology with height differences ranging from  $-35.9652 \mu\text{m}$  to  $4.71027 \mu\text{m}$ .

effectiveness in food preservation. Water barrier properties are particularly important, as they help maintain the moisture balance, texture, and overall stability of food products during

storage.<sup>28,47</sup> These characteristics are commonly evaluated through measurements of moisture content, WVP and oxygen permeability. The WVP of a film is largely governed by its

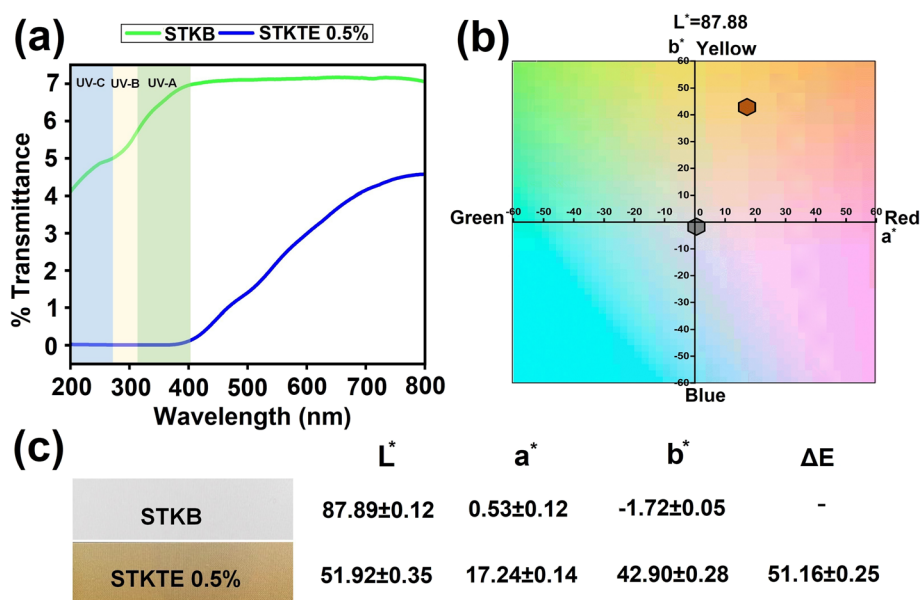


**Fig. 4** Optical and colorimetric properties of STKB and STKTE 0.5% films. (a) UV-visible transmittance spectra, where STKTE 0.5% exhibits significantly reduced transmittance across the UV region (UV-C to UV-A), indicating enhanced UV-shielding compared to STKB. (b) The CIE Lab\* color coordinates, with STKTE 0.5% shifting markedly toward the red-yellow quadrant, while STKB remains near the neutral centre. (c) Photographic images of both films and their corresponding colorimetric values. STKTE 0.5% shows a much lower lightness ( $L^*$ ) and higher chromaticity ( $a^*$ ,  $b^*$ ), resulting in a notable color difference ( $\Delta E = 51.16$ ) relative to STKB.



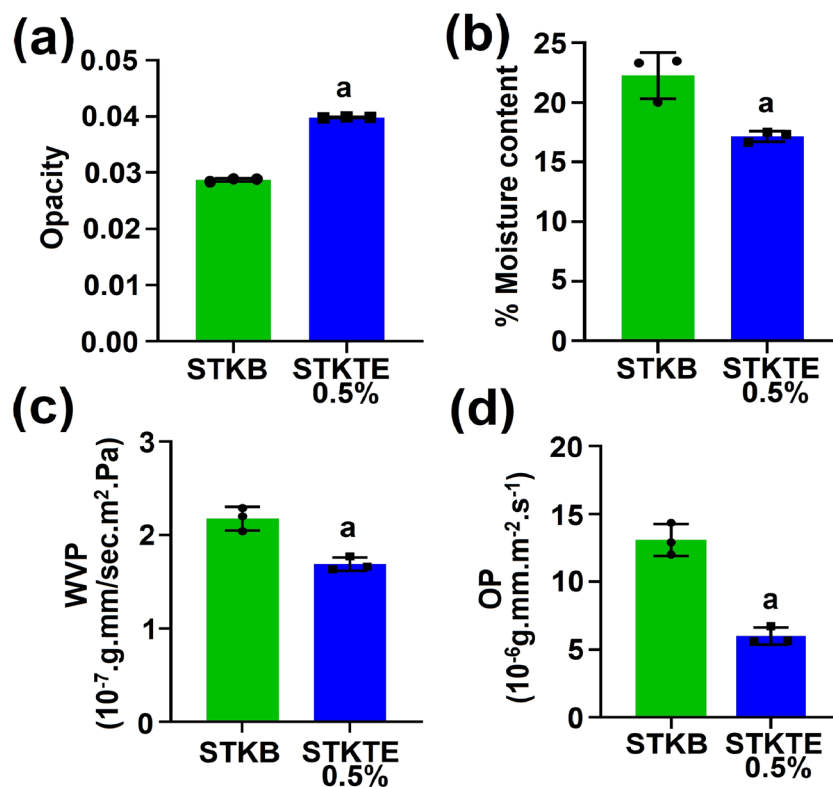


**Fig. 5** A comparison of the physical and barrier properties between STKB and STKTE 0.5% films. (a) The opacity of the films increased significantly with the addition of 0.5% TE, indicating higher light-blocking capability. (b) The moisture content was significantly reduced in the STKTE 0.5% films compared to STKB, suggesting improved hydrophobic characteristics. (c) The water vapor permeability (WVP) decreased in STKTE 0.5% films, indicating enhanced barrier properties against moisture. (d) The oxygen permeability (OP) was also significantly lower in the STKTE 0.5% films, reflecting better resistance to oxygen transmission. Data are presented as mean  $\pm$  standard deviation ( $n = 3$ ), and bars with "a" indicate statistically significant differences ( $p < 0.05$ ) from the STKB film.

thickness, degree of crosslinking, and polymer chain mobility. Additionally, oxygen exposure can accelerate undesirable processes such as lipid oxidation, discoloration, and microbial growth, ultimately leading to food spoilage.<sup>48</sup> Collectively, these factors are essential for preserving the freshness, sensory quality, and nutritional value of foods while extending their shelf life. Therefore, the developed films were assessed for these parameters to comprehensively evaluate their barrier performance.

The results revealed that the moisture content % of the STKTE 0.5% film ( $17.16 \pm 0.44\%$ ) was significantly reduced compared to the STKB film ( $22.28 \pm 1.94\%$ ) (Fig. 5b). The decrease in the moisture content % of the tea extract loaded (STKTE 0.5%) film was due to the inclusion of the hydrophobic constituents of TE, which lower the water adsorption capability of the film. Similar results were reported by Wen *et al.* in their study on pH-sensitive poly (vinyl alcohol) films incorporated with green tea extract.<sup>40</sup> Similarly, notable decreases in the WVP and OP of the STKTE 0.5% film were observed (Fig. 5c and d). Specifically, the STKTE 0.5% film exhibited a significantly lower WVP ( $1.68 \pm 0.07 \times 10^{-7}$  g mm s<sup>-1</sup> m<sup>2</sup> Pa) than the STKB film ( $2.17 \pm 0.12 \times 10^{-7}$  g mm s<sup>-1</sup> m<sup>2</sup> Pa). The WVP of the STKTE 0.5% film was decreased due to the addition of TE containing a bulky aromatic skeleton, which can obstruct the inner network of the tea extract loaded film (STKTE 0.5%),

corresponding to lower vapor affinity of the films.<sup>40,42</sup> The oxygen permeability of the films followed a similar trend to the WVP. The STKTE 0.5% film exhibited a significant decrease ( $5.97 \pm 0.63 \times 10^{-6}$  g mm m<sup>-2</sup> s<sup>-1</sup>) in the oxygen permeability as compared to the STKB film ( $13.07 \pm 1.18 \times 10^{-6}$  g mm m<sup>-2</sup> s<sup>-1</sup>). The TE present in the STKTE 0.5% film acted as a barrier that successfully inhibited the diffusion of oxygen molecules, which corresponds to lower oxygen permeability. Also, the crosslinking of the film materials reduced the free space present in the film, resulting in low OP values.<sup>14</sup> These findings indicated that the addition of 0.5% TE not only increases film opacity but also enhances the moisture resistance and gas barrier performance, making the modified film potentially more suitable for packaging applications.

**3.2.3. Molecular, solid state and thermal analysis of STKB and STKTE 0.5% films.** The FTIR spectra of the film and film components were analysed to understand the intermolecular interaction between the components of the films (Fig. 6a). The FTIR spectra of ST showed bands at  $3339$  cm<sup>-1</sup> and  $2929$  cm<sup>-1</sup> corresponding to the symmetric and asymmetric stretching vibrations of O-H and C-H groups. The absorption peak at  $991$  cm<sup>-1</sup> was attributed to the hydrogen bond formed by oxygen atoms on the ST glycosidic bond.<sup>5,23,49</sup> The FTIR spectrum of the PVA-PEG copolymer (KIR) showed a broad and intense absorption band between  $3600$  and  $3000$  cm<sup>-1</sup>, related to O-H



stretching vibrations, indicative of strong hydrogen bonding interactions. Two distinct peaks at  $2903\text{ cm}^{-1}$  and  $1439\text{ cm}^{-1}$  were attributed to asymmetric  $\text{CH}_2$  stretching and  $\text{CH-O-H}$  bending vibrations, contributing to the polymeric backbone structure. Additionally, two characteristic peaks at  $1241\text{ cm}^{-1}$  and  $1092\text{ cm}^{-1}$  correspond to  $\text{C-O-C}$  stretching of the alkyl ether group and  $\text{C-O}$  stretching vibrations, respectively.<sup>17,50</sup> The FTIR spectra of TE demonstrated absorption at  $1315\text{ cm}^{-1}$  and  $1446\text{ cm}^{-1}$ , which was attributed to  $\text{C-H}$  stretching, and a peak at  $1647\text{ cm}^{-1}$  was attributed to  $\text{C=C}$  stretching.<sup>40</sup> The FTIR spectra of the STKB and STKTE 0.5% film exhibited broadening and shifting of peaks of film components in the region of  $3700\text{--}3000\text{ cm}^{-1}$  and  $1500\text{--}1800\text{ cm}^{-1}$  demonstrating possible hydrogen bonding linkage between the film polymers.

The crystal structures of the ST, PVA-PEG copolymer (KIR), TE, STKB, and STKTE 0.5% were determined using XRD analysis (Fig. 6b). The XRD pattern of ST exhibited a high intensity peak at  $17^\circ$  and low intensity peaks at  $15^\circ$ ,  $22.6^\circ$  and  $23.7^\circ$ , demonstrating its partial crystalline nature.<sup>5,23</sup> On the other hand, the diffractogram of KIR exhibited only a diffuse pattern, with peaks at  $19.3^\circ$  and  $22.7^\circ$  ( $2\theta$ ), typical of semi-crystalline polymeric structures.<sup>51</sup> Similarly, the XRD spectra of TE demonstrated its partial amorphous nature due to the presence of numerous components including fibres, tea polyphenols and catechins. Further, the XRD diffractograms of the film samples (STKB and STKTE 0.5%) demonstrated diffuse and halo spectra, revealing amorphization of the film components. This transition towards an amorphous structure reflects strong interfacial interactions between the components, which may enhance material uniformity and performance.

The thermal stability of the developed films was analyzed by thermogravimetric analysis. TGA thermograms of all samples demonstrated multi-step degradation, typically involving initial moisture loss followed by the decomposition of the organic matrix (Fig. 6c). Specifically, degradation of ST was initiated at  $246.1^\circ\text{C}$  to  $378.5^\circ\text{C}$  and  $378.5^\circ\text{C}$  to  $548.7^\circ\text{C}$ , corresponding to 52.1% and 27.21% weight loss with a residual weight of 7.19%,

respectively.<sup>25,52</sup> The TGA profile of the PVA-PEG copolymer (KIR) exhibited a distinct two-step degradation pattern.<sup>53</sup> The initial stage showed a minor weight loss of approximately 1.3% below  $150^\circ\text{C}$ , corresponding to the evaporation of physically adsorbed and bound water molecules. The primary decomposition phase occurred between  $163^\circ\text{C}$  and  $432.6^\circ\text{C}$ , resulting in a weight loss of about 81.33%, which can be attributed to the degradation of organic constituents and partial cleavage of the polymer backbone. Subsequent degradation events between  $432.6\text{--}483.2^\circ\text{C}$ , and  $483.2\text{--}550^\circ\text{C}$ , contributed additional weight losses of 6.17% and 10.6%, respectively. The thermogram of TE displayed a broad degradation band beginning at around  $150^\circ\text{C}$ , with a peak near  $200^\circ\text{C}$  to  $392^\circ\text{C}$  corresponding to 95% weight loss. This transition is attributed to the thermal decomposition of glycosylated catechins, where the attached sugars undergo caramelization upon heating. Additionally, the partial degradation of catechins, leading to the formation of gallic acid and subsequent polymerization of phenolic compounds, contributes to this thermal event. The degradation extended over a wide temperature range, with a final stage observed beyond  $340^\circ\text{C}$ , corresponding to the thermal decomposition of cellulose components present in the TE.<sup>40</sup>

The thermal stability of the film samples improved upon the incorporation of TE in the film components, as observed in the STKTE 0.5% curves, which show delayed onset of degradation from  $200^\circ\text{C}$  (in TE) to  $229^\circ\text{C}$ . Moreover, the TGA curve of STKTE 0.5% demonstrated a gradual increase in weight loss despite the sharp increase in degradation observed in the TE curve. This enhancement can be attributed to the reinforcing effect and thermal barrier properties imparted by the additives.

Overall, the combined FTIR, XRD, and TGA results confirm the successful integration of the PVA-PEG copolymer (KIR) and TE into the ST matrix, leading to chemical interactions, reduced crystallinity, and improved thermal stability. These modifications suggest that the composite film enhanced the structural homogeneity and thermal resistance compared to the unmodified samples.

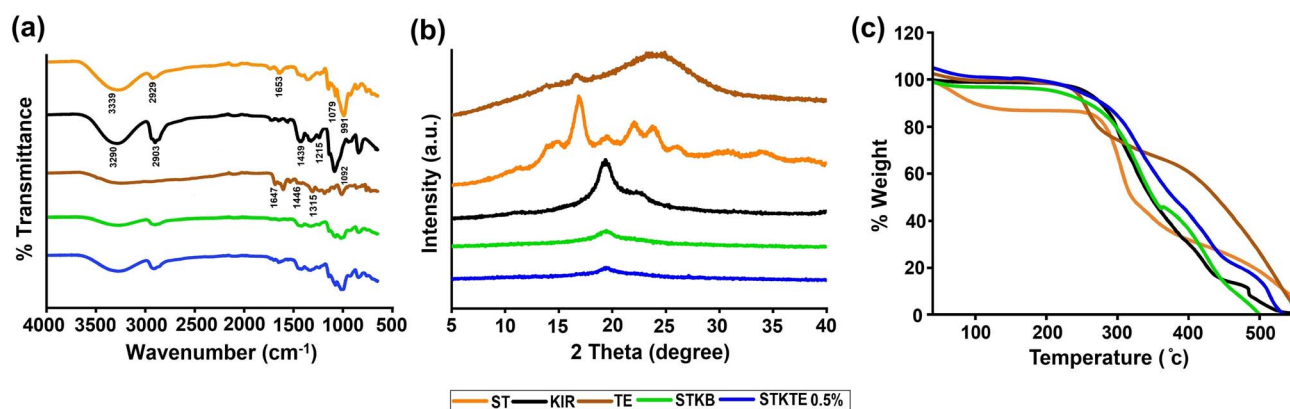


Fig. 6 Solid state characterization of ST, KIR, TE, STKB, and STKTE 0.5% samples. (a) Fourier-transform infrared (FTIR) spectra showing characteristic functional groups and chemical interactions among the materials. (b) X-ray diffraction (XRD) patterns highlight the crystallinity and structural changes of the samples. (c) Thermogravimetric analysis (TGA) curves displaying thermal stability and decomposition profiles as a function of temperature.



### 3.3. Antioxidant activity and biocompatibility of STKB and STKTE 0.5% films

Antioxidant ability (free radical scavenging activity) is crucial for food packaging films, as free radicals generated in food can cause oxidation and spoilage of food. The DPPH radical scavenging activity is important to estimate the antioxidant properties of film samples. The results demonstrated that the DPPH scavenging activity of the STKTE 0.5% film exhibited a concentration dependent increase as compared to the STKB film, with 84% scavenging at the highest concentration ( $1000 \mu\text{g mL}^{-1}$ ) (Fig. 7a). However, the STKB film showed only 7% scavenging at the highest concentration ( $1000 \mu\text{g mL}^{-1}$ ). The addition of TE improved the antioxidant potential of the film (STKTE 0.5%), due to the presence of phenolic compounds present in the TE. The TE components are known to disrupt chain oxidation reaction, releasing hydrogen atoms and acting as a receptor for free radicals.<sup>13,27,54</sup> This suggested that the addition of TE significantly influenced the antioxidant activity of the films.

To determine the cytocompatibility of the developed films (STKB and STKTE 0.5%), *in vitro* biocompatibility was analysed using the L929 mouse fibroblast cell line. The film samples were incubated with fibroblast cells followed by MTT assay to determine cell viability. In both films (STKB and STKTE 0.5%), the cell viability observed was more than 90%, suggesting that the films are biocompatible and non-toxic to cells (Fig. 7b). Despite the incorporation of TE, the STKTE 0.5% film sample maintained high cell compatibility, demonstrating that neither

its concentration nor its incorporation method induced any adverse cellular response.<sup>21,55</sup> The excellent biocompatibility of these films supports their potential role for interaction with biological tissues extending their application beyond the food packaging.

### 3.4. Tea extract migration analysis

In general, the release/migration of active components from the film is critical for providing effective functional attributes to the film. This migration depends upon the type of food preserved in the packaging material and its rate depends upon compatibility between the film polymer, food simulant and active component.<sup>37</sup> Therefore, the migration of TE from STKTE 0.5% films was analyzed in three different food simulants (3% acetic acid, 95% ethanol and water) (Supplementary Table S1). The results of the migration study revealed that the film in the 3% acetic acid ( $79.7 \pm 2.0\%$ ) and water simulant ( $77.3 \pm 2.7\%$ ) showed maximum release/migration of TE from film to solution. However, the film incubated in 95% ethanol demonstrated  $51.5 \pm 4.4\%$  migration of TE, possibly because of the limited solubility of starch in ethanol. Further, the DPPH assay of the simulant solution also confirmed the effective migration and retention of the antioxidant activity of the films (Supplementary Fig. S1). Specifically, antioxidant assay results revealed that the films in 3% acetic acid ( $80.1 \pm 0.2\%$ ) and water ( $72.7 \pm 0.2\%$ ) demonstrated the highest DPPH scavenging activity, equivalent to that of the STKTE 0.25% film without simulant treatment, in

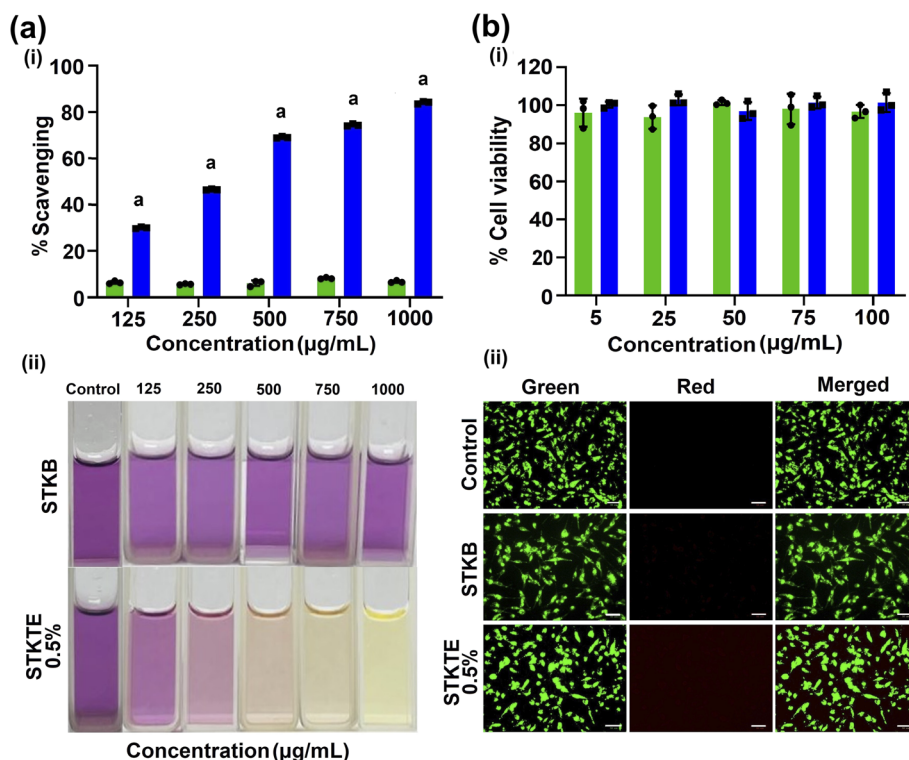


Fig. 7 Antioxidant activity and biocompatibility of STKB and STKTE 0.5% film. (a) DPPH scavenging assay shows dose-dependent antioxidant activity for STKTE (0.5%) film, significantly higher than STKB at all concentrations ( $p < 0.05$ ). (b-i) The L929 cell viability graph and (b-ii) fluorescence images demonstrate predominantly live cells (green) supporting the biocompatibility of both films (STKB and STKTE 0.5%). The scale bar in the microscopy images is  $50 \mu\text{m}$ .



comparison to the film in 95% ethanol simulant ( $60.1 \pm 0.2\%$ ). The higher antioxidant activity in acetic acid and water may be because of the higher solubility of the film in these simulants in comparison to ethanol. ST alone is usually less soluble in water, but the incorporation of the PVA-PEG copolymer increased its solubility by forming hydroxyl groups and allows the antioxidant compounds to be released more effectively from the film samples.<sup>56</sup> Similar results were obtained in a study on mixing potato starch with PVA, which results in the formation of hydrophilic films and increases the solubility of the films in water, mainly because of an increase in the number of -OH groups.<sup>57</sup>

### 3.5. Antibacterial activity of STKB and STKTE 0.5% films

The antibacterial properties of the developed films can inhibit the growth of potential foodborne pathogens, and thereby limit foodborne illnesses and prolong food shelf-life. The antibacterial efficiency of the developed films was tested against two bacterial strains, *S. aureus* (Gram-positive) and *E. coli* (Gram-negative) bacteria, and determined by the colony forming unit (CFU per mL) method (Fig. 8). The control and STKB film exhibited intense bacterial growth in comparison to STKTE 0.5% against both the bacterial strains (*S. aureus* and *E. coli*). Specifically, the STKTE 0.5% film showed  $7.9 \times 10^6$  CFU per mL against *S. aureus* and  $3.3 \times 10^6$  CFU per mL against *E. coli*, which indicates that the STKTE 0.5% film exhibited a significant antibacterial effect against *E. coli* as compared to *S. aureus* (Fig. 8). The results demonstrated that the developed STKTE 0.5% film showed promising inhibition of growth of both the bacterial strains in comparison to the STKB film. The antibacterial properties of the STKTE 0.5% film can be attributed to the incorporation of the TE, which contains polyphenols, and has

the potential to inhibit the growth of a wide variety of bacteria, especially Gram-positive and Gram-negative species.<sup>13</sup> The observed results are supported by the findings of Lie *et al.*, which reported the significant inhibition of *E. coli* compared to *S. aureus* at equivalent concentrations of TE.<sup>24</sup>

### 3.6. Fresh cut apple preservation

The ability of the STKB and STKTE 0.5% films to preserve fresh cut apple was examined by monitoring several quality parameters, *viz.* Visual appearance, color parameters, % weight loss, pH and BI.<sup>32</sup> In terms of visual appearance, the fruits packed in the STKTE 0.5% film effectively maintained their appearance until the 5th day of the experiment followed by the STKB, PE and control groups (Fig. 9a). Moreover, the color parameters ( $L^*$ ,  $a^*$  and  $b^*$  values) of the apple cubes were in agreement with the visual appearance, confirming the color changes during storage (Fig. 9b). Furthermore, the browning index of the apple samples was also evaluated, and the results demonstrated that the browning index of the apple cubes was highest in the control sample as the fruit cubes were not protected. However, in the case of covered fruit cubes the browning index was decreased in the order PE > STKB > STKTE 0.5% (Fig. 9c). The possible cause of fruit browning could be polyphenol oxidation to produce quinones, which react to generate brown/black pigments.<sup>33,58</sup>

The weight loss of stored apple cubes was also estimated over a period of 5 days and it was observed that the weight loss was at a maximum ( $57.1 \pm 10.4$ ) in the control group (uncovered apple cubes). In contrast, the covered apple cubes exhibited a lower weight loss for PE ( $52.0 \pm 10.7$ ), followed by STKB ( $30.2 \pm 6.6$ ) and then STKTE 0.5% ( $28.6 \pm 6.4$ ) (Fig. 9d). The weight loss observed in all the groups is likely to be associated with the rapid increase in respiration just after the cutting of the fruit.

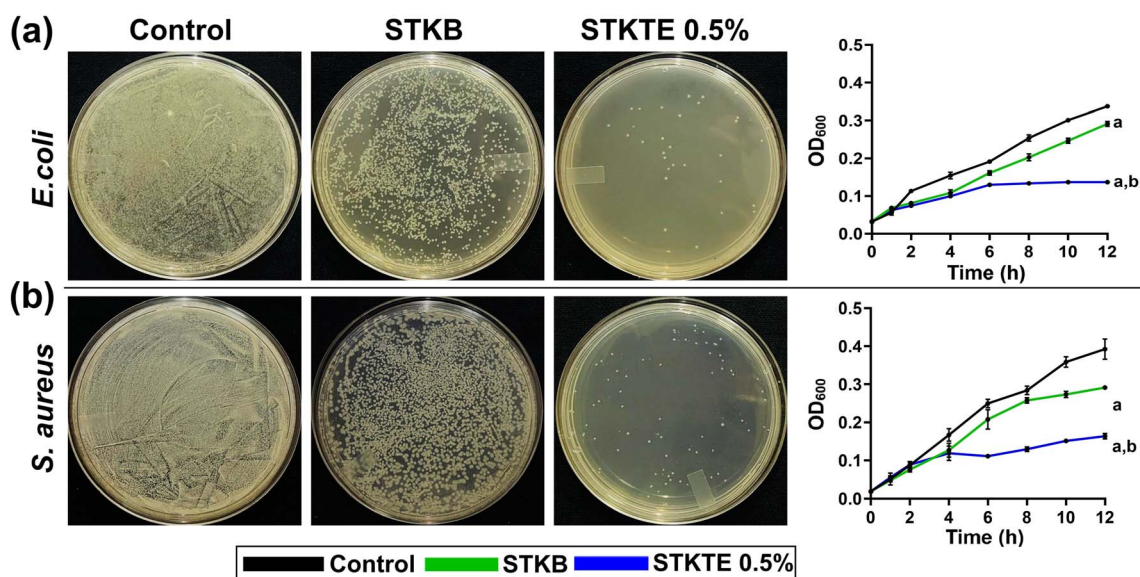


Fig. 8 Antibacterial effects of STKB and STKTE 0.5% against *S. aureus* and *E. coli*. (a) Representative agar plates of *E. coli* demonstrating bacterial inhibition with reduced colony formation and growth curves (OD<sub>600</sub>) demonstrating that both films reduce bacterial growth over 12 h compared to the control sample, with STKTE 0.5% exhibiting stronger inhibition. (b) Representative agar plates of *S. aureus* demonstrating bacterial inhibition, with reduced colony formation and growth curves (OD<sub>600</sub>) over 12 h (a)  $p < 0.05$  vs. control; (b)  $p < 0.05$  vs. STKB).



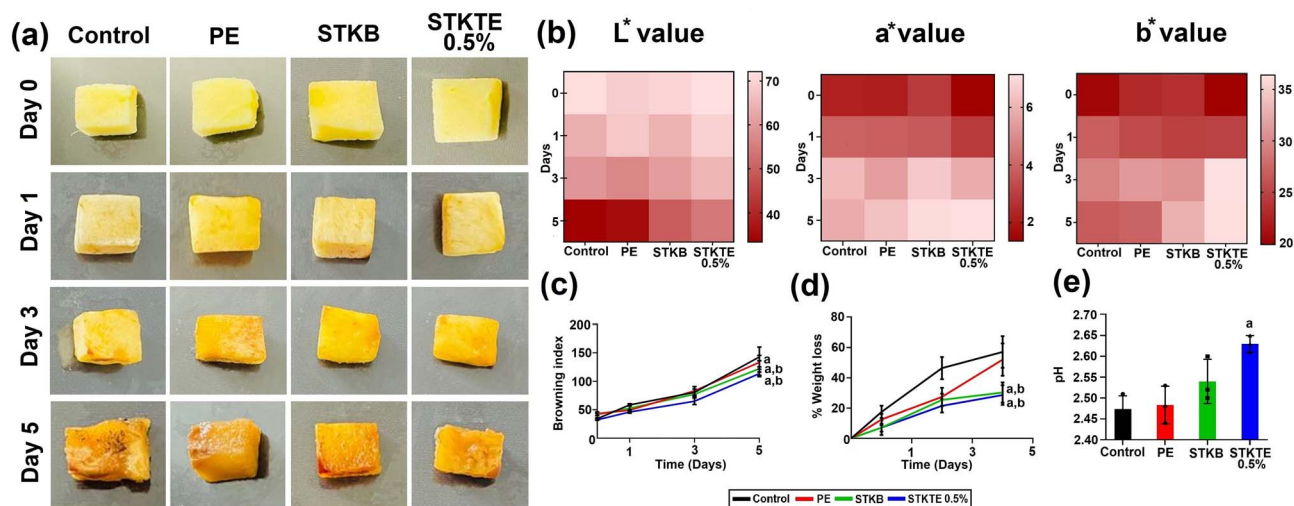


Fig. 9 Effects of different treatments on the quality of fresh-cut apples over 5 days of storage. (a) The representative images of apple cubes showing visual appearance demonstrated that STKTE 0.5% best preserved the color, while the control sample showed the most browning. (b) Heatmaps of color values ( $L^*$ ,  $a^*$ , and  $b^*$ ) indicate that STKTE 0.5% retained lightness and color better than other treatments. (c) The browning index increased in all samples, but was lowest in STKTE 0.5% ( $n = 3$ ). (d) Weight loss was highest in the control sample and lowest in STKTE 0.5%, indicating improved moisture retention. (e) Graph depicting the change in pH of the fruit after storage for 5 days. (a)  $p < 0.05$  vs. control; (b)  $p < 0.05$  vs. STKB).

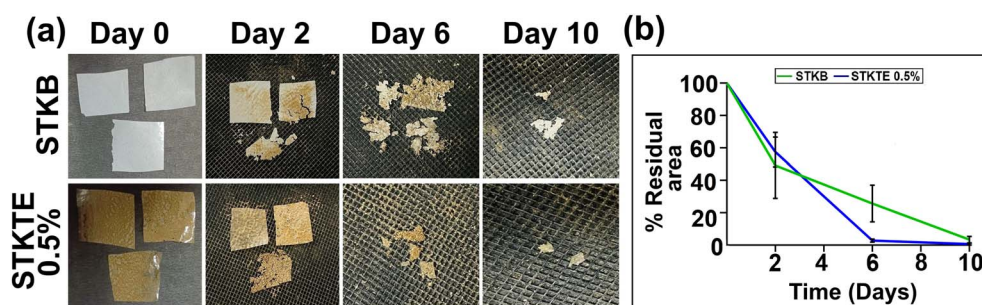


Fig. 10 Soil burial test assessment of STKB and STKTE 0.5% films over time. (a) Representative images showing the physical degradation of STKB and STKTE 0.5% films over a 10-day period. (b) Quantitative analysis of % residual area for STKB (green line) and STKTE 0.5% (blue line) films over time. Data represent mean  $\pm$  standard deviation ( $n = 3$ ). STKTE 0.5% films exhibited slightly faster degradation compared to STKB film.

Moreover, since moisture loss is directly associated with film permeability, the weight loss results can be interpreted on the basis of WVP values.<sup>58,59</sup> The film with a lower WVP (STKTE 0.5%) exhibited the lowest weight loss, whereas the STKB film with a higher WVP showed greater weight loss than the STKTE 0.5% film.

The pH serves as a key indicator of fruit freshness and spoilage. The decrease in apple pH during storage is primarily attributed to the accumulation of acidic metabolites, enzymatic breakdown of cell wall components, and potential microbial fermentation. Together, these processes increase the fruit's overall acidity, signalling progressive deterioration in quality.<sup>32</sup> Therefore, the pH of the apple sample was estimated at the end of the experiment, revealing that the pH in the control group was the lowest ( $2.47 \pm 0.03$ ) compared to the other groups. The STKTE 0.5% group was found to be the best to maintain the pH ( $2.63 \pm 0.02$ ) of the fruits in comparison to the blank sample ( $2.53 \pm 0.05$ ) and commercial packaging film ( $2.48 \pm 0.04$ ) (Fig. 9e).

### 3.7. Soil burial test assessment

The physical disintegration assessment of the STKB and STKTE 0.5% films was carried out using the soil burial method for a period of 10 days.<sup>34</sup> The STKTE 0.5% film showed significant reduction in film area with a residual area of  $0.6 \pm 0.6\%$  as compared to the STKB film ( $3.4 \pm 2.0\%$ ), confirming its high vulnerability towards microbial degradation and breakdown under environmental conditions (Fig. 10). Overall, both the films, STKB and STKTE 0.5%, showed the potential to serve as sustainable alternatives to conventional food packaging materials.

## 4. Conclusion

In summary, this study presents the successful development of biodegradable and functional films based on starch and a PVA-PEG (Kollicoat IR) copolymer incorporated with green tea extract (TE) as a natural bioactive additive. The incorporation of 0.5% w/v TE markedly enhanced the mechanical strength, water



contact angle and barrier properties of the films, demonstrating superior performance compared to the blank STKB film. The structural and thermal analyses (SEM, 3D profilometry, FTIR, XRD, and TGA) confirmed improved film uniformity, strong intermolecular interactions, and enhanced thermal stability upon TE addition. The developed films exhibited enhanced antioxidant and antibacterial activities, effectively inhibiting *E. coli* and *S. aureus*, while maintaining cytocompatibility in L929 fibroblast cells. The application of the films for packaging fresh-cut apples significantly reduced browning, weight loss, and pH decrease, indicating extended shelf life and improved preservation quality. Moreover, the films displayed rapid physical disintegration within 10 days under soil burial conditions, confirming their environmental sustainability. However, the long-term stability and food-grade safety assessments are required for PVA-PEG copolymer (Kollicoat IR) before large-scale commercial applications. Overall, the developed ST/PVA-PEG/TE films present a promising green alternative to conventional plastic packaging, combining biodegradability, bioactivity, and functional performance suitable for food preservation and sustainable packaging applications.

## Author contributions

Neha Rana: writing – original draft, methodology, investigation, data curation, formal analysis. Ruchika: methodology, investigation, writing – original draft, formal analysis. Ankit Saneja: writing – review & editing, supervision, project administration, funding acquisition, conceptualization.

## Conflicts of interest

The authors declare that they have no known competing financial interests or personal relationships that could have appeared to influence the work reported in this paper.

## Data availability

Data supporting the findings of this study are available within the article.

Supplementary information (SI): supplementary information includes tables of the percent migration of tea extract from the STKTE 0.5% film and figures showing the DPPH assay of film samples after the migration study conducted for 10 days in different food simulants (3% acetic acid, water and 95% ethanol). See DOI: <https://doi.org/10.1039/d5fb00838g>.

## Acknowledgements

The authors acknowledge the Director, CSIR – Institute of Himalayan Bioresource Technology, for his support. The authors thank the Council of Scientific and Industrial Research (CSIR), New Delhi, for financial assistance under the MLP-204 and CSPS24/RDSF/IHBT/IHP24/09 project. Fig. 1 and the graphical abstract were created using BioRender.com. During the preparation of this article, the author(s) used “Grammarly” to improve the language of the manuscript with appropriate

caution. The author(s) reviewed and edited the content after using the tool and take full responsibility for the final version of the published article. The manuscript bears institutional communication number 6003.

## References

- H. Baniyadi, R. Abidnejad, M. Fazeli, J. Niskanen and E. Lizundia, *Mater. Sci. Eng. R Rep.*, 2026, **167**, 101128.
- M. Anwar, M. E. Konnova and S. Dastgir, *RSC Sustain.*, 2025, **3**, 3724–3840.
- W. Zhang, J. Yang, M. Ghasemlou, Z. Riahi, A. Khan, G. Goksen, Y. Zhang and J.-W. Rhim, *Mater. Sci. Eng. R Rep.*, 2025, **166**, 101068.
- P. Kalita, N. S. Bora, B. Gogoi, A. Goswami, L. Pachau, P. J. Das, D. Baishya and S. Roy, *Food Chem.*, 2025, 143793.
- Y. Ma, H. Zhao, Q. Ma, D. Cheng, Y. Zhang, W. Wang, J. Wang and J. Sun, *Food Packag. Shelf Life*, 2022, **31**, 100793.
- A. Khan, P. Ezati and J.-W. Rhim, *ACS Appl. Bio Mater.*, 2023, **6**, 1294–1305.
- H. Deng, J. Su, W. Zhang, A. Khan, M. A. Sani, G. Goksen, P. Kashyap, P. Ezati and J.-W. Rhim, *Int. J. Biol. Macromol.*, 2024, **273**, 132926.
- X. Zhao, Y. Wang, X. Chen, X. Yu, W. Li, S. Zhang, X. Meng, Z.-M. Zhao, T. Dong and A. Anderson, *Matter*, 2023, **6**, 97–127.
- A. A. Hunashyal, S. P. Masti, M. P. Eelager, O. J. D'souza, L. K. Kurabetta, M. N. Gunaki, S. Madihalli, J. P. Pinto, M. B. Megalamani and R. B. Chougale, *Next Nanotechnol.*, 2025, **8**, 100292.
- S. Phattarateera, R. Wungpunya, S. Thongkhlaeo, L. Tatong, C. Thongpin and P. Threepopnatkul, *J. Polym. Res.*, 2025, **32**, 390.
- M. Sharma, P. Beniwal and A. P. Toor, *Mater. Chem. Phys.*, 2022, **291**, 126652.
- C. Xu, S. Zhou, H. Song, H. Hu, Y. Yang, X. Zhang, S. Ma, X. Feng, Y. Pan and S. Gong, *Nano Today*, 2023, **52**, 101990.
- P. Shan, K. Wang, F. Yu, L. Yi, L. Sun and H. Li, *Colloids Surf., A*, 2023, **662**, 131013.
- J. R. Ansari, K. Park and J. Seo, *Food Packag. Shelf Life*, 2025, **48**, 101460.
- J. Wu, S. Chen, S. Ge, J. Miao, J. Li and Q. Zhang, *Food Hydrocoll.*, 2013, **32**, 42–51.
- M. A. Andrade, C. H. Barbosa, M. A. Cerqueira, A. G. Azevedo, C. Barros, A. V. Machado, A. Coelho, R. Furtado, C. B. Correia, M. Saraiva, F. Vilarinho and A. S. Silva, *Food Packag. Shelf Life*, 2023, **36**, 101041.
- A. J. Mali, S. Patil and B. Chellampillai, *J. Polym. Res.*, 2022, **29**, 130.
- A. L. Vicario, M. G. Garcia, N. A. Ochoa and E. Quiroga, *Food Hydrocolloids*, 2024, **153**, 110009.
- A. Aragón-Gutiérrez, L. Higuera-Contreras, G. López-Carballo, A. Gómez-García, M. Gallur, D. López, R. Gavara and P. Hernández-Muñoz, *Food Packag. Shelf Life*, 2024, **46**, 101355.
- N. Khan and A. Saneja, *J. Mol. Struct.*, 2025, 142652.
- S. Ruchika, S. Kumar, R. Kumar, S. K. Yadav and A. Saneja, *Int. J. Biol. Macromol.*, 2025, **293**, 139241.



- 22 N. Deng, Z. Hu, H. Li, C. Li, Z. Xiao, B. Zhang, M. Liu, F. Fang, J. Wang and Y. Cai, *Int. J. Biol. Macromol.*, 2024, **260**, 129340.
- 23 Y. Wang, H. Zhang, Y. Zeng, M. A. Hossen, J. Dai, S. Li, Y. Liu and W. Qin, *Food Packag. Shelf Life*, 2022, **33**, 100837.
- 24 Y. Lei, H. Wu, C. Jiao, Y. Jiang, R. Liu, D. Xiao, J. Lu, Z. Zhang, G. Shen and S. Li, *Food Hydrocolloids*, 2019, **94**, 128–135.
- 25 K. Yogananda, E. Ramasamy and D. Rangappa, *Ionics*, 2019, **25**, 6035–6042.
- 26 S. R. Kanatt, M. Rao, S. Chawla and A. Sharma, *Food Hydrocoll.*, 2012, **29**, 290–297.
- 27 M. Abdin, A. A. Metwally, M. Younis, M. Khalil and S. G. Arafa, *Food Chem.*, 2025, 147089.
- 28 J. Chen, X. Zhang, H. Lin, G. Chen, W. Zhang and D.-P. Yang, *Chem. Eng. J.*, 2025, **511**, 162184.
- 29 C. L. de Dicastillo, M. del Mar Castro-López, J. M. López-Vilariño and M. V. J. F. r. i. González-Rodríguez, *Food Res. Int.*, 2013, **53**, 522–528.
- 30 F. S. Mortazavi Moghadam, S. Rasouli and F. A. Mortazavi Moghadam, *ACS Food Sci. Technol.*, 2025, **5**, 1024–1041.
- 31 R. Podgórski, M. Wojański and T. Ciach, *Sci. Rep.*, 2022, **12**, 9047.
- 32 T. Almeida, A. Karamysheva, B. F. Valente, J. M. Silva, M. Braz, A. Almeida, A. J. Silvestre, C. Vilela and C. S. Freire, *Food Hydrocolloids*, 2023, **144**, 108934.
- 33 L. Jiang, F. Wang, X. Xie, C. Xie, A. Li, N. Xia, X. Gong and H. Zhang, *Int. J. Biol. Macromol.*, 2022, **209**, 1307–1318.
- 34 M. Liu, H. Chen, F. Pan, X. Wu, Y. Zhang, X. Fang, X. Li, W. Tian and W. Peng, *Carbohydr. Polym.*, 2024, **343**, 122445.
- 35 T. C. Vianna, C. O. Marinho, L. M. Júnior, S. A. Ibrahim and R. P. Vieira, *Int. J. Biol. Macromol.*, 2021, **182**, 1803–1819.
- 36 R. K. Sidhu, C. Riar and S. Singh, *Sustainable Food Technol.*, 2026, DOI: [10.1039/D5FB00606F](https://doi.org/10.1039/D5FB00606F).
- 37 T. Y. Feng, M. N. Hidayah, F. H. Lyn and Z. N. Hanani, *Sustainable Food Technol.*, 2025, **3**, 1986–1995.
- 38 R. K. Gupta, P. Guha and P. Srivastav, *Plasma Processes Polym.*, 2024, **21**, 2400047.
- 39 Z. Wang, C. Xu, L. Qi and C. Chen, *Trends Chem.*, 2024, **6**, 314–331.
- 40 H. Wen, Y.-I. Hsu, T.-A. Asoh and H. Uyama, *Polym. Degrad. Stabil.*, 2020, **178**, 109215.
- 41 Z. Wu, C. Tong, J. Zhang, J. Sun, H. Jiang, M. Duan, C. Wen, C. Wu and J. Pang, *Int. J. Biol. Macromol.*, 2021, **192**, 323–330.
- 42 H. Wu, Y. Lei, R. Zhu, M. Zhao, J. Lu, D. Xiao, C. Jiao, Z. Zhang, G. Shen and S. Li, *Food Hydrocolloids*, 2019, **90**, 41–49.
- 43 A. Sadeghi, S. M. A. Razavi and D. Shahrampour, *Int. J. Biol. Macromol.*, 2022, **205**, 341–356.
- 44 T. S. Awad, D. Asker and B. D. Hatton, *ACS Appl. Mater. Interfaces*, 2018, **10**, 22902–22912.
- 45 A. H. Hashem, M. E. El-Naggar, A. M. Abdelaziz, S. Abdelbary, Y. R. Hassan and M. S. Hasanin, *Int. J. Biol. Macromol.*, 2023, **249**, 126011.
- 46 W. Zhang, H. Jiang, J.-W. Rhim, J. Cao and W. Jiang, *Crit. Rev. Food Sci. Nutr.*, 2022, **63**, 288–301.
- 47 F. N. Eze, R. C. Eze, S. Singh and K. E. Okpara, *Int. J. Biol. Macromol.*, 2024, **278**, 134914.
- 48 Q. Hua, Z. Huang, J. Gou, H. Zhang, I. Therrien, J. Wu, Y. Liang and S. Rennecker, *Chem. Eng. J.*, 2024, **499**, 156139.
- 49 R. Abedi-Firoozjah, N. Chabook, O. Rostami, M. Heydari, A. Kolahdouz-Nasiri, F. Javanmardi, K. Abdolmaleki and A. M. Khaneghah, *Polym. Test.*, 2023, **118**, 107903.
- 50 P. Desai and B. Chatterjee, *ACS omega*, 2023, **8**, 45337–45347.
- 51 S. Janssens, H. N. de Armas, J. P. Remon and G. Van den Mooter, *Eur. J. Pharmaceut. Sci.*, 2007, **30**, 288–294.
- 52 B. Schmidt, K. Kowalczyk and B. Zielinska, *Materials*, 2021, **14**, 1498.
- 53 D. Kramarczyk, J. Knapik-Kowalczyk, M. Kurek, W. Jamróz, R. Jachowicz and M. Paluch, *Pharmaceutics*, 2023, **15**, 799.
- 54 V. Hemmati, F. Garavand, N. Khorshidian, I. Cacciotti, M. Goudarzi, M. Chaichi and B. K. Tiwari, *Food Biosci.*, 2021, **44**, 101348.
- 55 E. P. Bavi, E. Shakerinasab, H. Hamidinezhad and E. Nazifi, *Int. J. Biol. Macromol.*, 2023, **224**, 1183–1195.
- 56 S. Patil, A. K. Bharimalla, A. Mahapatra, J. Dhakane-Lad, A. Arputharaj, M. Kumar, A. Raja and N. Kambli, *Food Biosci.*, 2021, **44**, 101352.
- 57 C. A. Gómez-Aldapa, G. Velazquez, M. C. Gutierrez, E. Rangel-Vargas, J. Castro-Rosas and R. Y. Aguirre-Loredo, *Mater. Chem. Phys.*, 2020, **239**, 122027.
- 58 M. El Mouzahim, E. Eddarai, S. Eladaoui, A. Guenbour, A. Bellaouchou, A. Zarrouk and R. Boussen, *Int. J. Biol. Macromol.*, 2023, **233**, 123430.
- 59 Y. Guan, Y. Ji, X. Yang, L. Pang, J. Cheng, X. Lu, J. Zheng, L. Yin and W. Hu, *LWT*, 2023, **175**, 114478.

